

## Iron(III) removal from aqueous solution using MCM-41 ceramic composite membrane

Ashim Kumar Basumatary<sup>1</sup>, R. Vinoth Kumar<sup>1</sup>,  
Kannan Pakshirajan<sup>2</sup> and G. Pugazhenthir<sup>\*1</sup>

<sup>1</sup> Department of Chemical Engineering, Indian Institute Technology Guwahati, Guwahati 781039, Assam, India

<sup>2</sup> Department of Biosciences and Bioengineering, Indian Institute Technology Guwahati,  
Guwahati 781039, Assam, India

(Received January 23, 2016, Revised July 02, 2016, Accepted July 24, 2016)

**Abstract.** Mesoporous MCM-41 was deposited on an inexpensive disk shaped ceramic support through hydrothermal technique for ultrafiltration of Fe<sup>3+</sup> from aqueous solution. The ceramic support was fabricated using uni-axial compaction technique followed by sintering at 950°C. The characteristics of MCM-41 powder as well as the composite membrane were examined by X-ray diffraction (XRD), thermogravimetric analysis (TGA), field emission scanning electron microscope (FESEM), porosity and pure water permeation test. The XRD result revealed the good crystallinity and well-resolved hexagonally arranged pore geometry of MCM-41. TGA profile of synthesized MCM-41 zeolite displayed the three different stepwise mechanisms for the removal of organic template. The formation of MCM-41 on the porous support was verified by FESEM analysis. The characterization results clearly indicated that the accumulation of MCM-41 by repeated coating on the ceramic disk directs to reduce the porosity and pore size from 47% to 23% and 1.0 to 0.173 μm, respectively. Moreover, the potential of the fabricated MCM-41 membrane was investigated by ultrafiltration of Fe<sup>3+</sup> from aqueous stream at various influencing parameters such as applied pressure, initial feed concentration and pH of solution. The maximum rejection 85% was obtained at applied pressure of 276 kPa and the initial feed concentration of 250 ppm at pH 2.

**Keywords:** ultrafiltration; FeCl<sub>3</sub>; zeolite membrane; MCM-41; hydrothermal

### 1. Introduction

Membrane separation processes have emerged as a promising technology during the past few decades and drawing world-wide attention among the research communities, especially in the field of separation technology (Nandi *et al.* 2008). Besides the membrane processes, inorganic membranes have generated a much interest in separation applications and catalytic reactions because of their unique advantageous characteristics. Inorganic membranes hold higher thermal and chemical stability, mechanical strength, longer life and good de-fouling properties in comparison with organic/polymeric membranes (Kumar *et al.* 2015a). Especially, the extensive development of zeolite supported membranes confers its certain advantageous properties such as higher mechanical and thermal stability, uniform pore size and channels, larger interior surface area and active sites (Wang *et al.* 2013). Moreover, the pore size and surface activity of the zeolite

---

\*Corresponding author, Professor, E-mail: [pugal@iitg.ernet.in](mailto:pugal@iitg.ernet.in)

supported membrane can be altered by selecting an appropriate type of zeolite.

Heavy metals including, copper (Cu), cadmium (Cd), chromium (Cr), lead (Pb), iron (Fe), zinc (Zn) and Mercury (Hg) have drawn significant concern in the field of wastewater treatment due to their high toxicity and their tendency to accumulate in living organisms (Chougui *et al.* 2014, Kasim *et al.* 2016, Urbanowska and Kabsch-Korbutowicz 2016). These are non-biodegradable in environment and considered as micro-pollutants. Several techniques such as reduction, lime precipitation, extraction and activated carbon adsorption are being employed to eliminate these pollutants from the contaminated water (Gzara 2001). Regrettably, the conventional techniques are incapable to minimizing the concentration of metals up to the permissible discharge limit (Cu: 0.05 mg/L; Cd: 0.003 mg/L; Cr: 0.05 mg/L; Pb: 0.01 mg/L; Fe: 0.3 mg/L; Zn: 5 mg/L and Hg: 0.001 mg/L). The ion-exchange and reverse osmosis can reduce the concentration level of the pollutants up to a tolerable limit; however, these processes are expensive. In general, inorganic pollutants contain charge carrying metal ions, which in turn to facilitate the incorporation of charged membranes to separate these ions (Shukla and Kumar 2005). Therefore, the development of new variety of ceramic materials with facile synthesis method could facilitate to attain ceramic membrane with charged selective layers. Wu *et al.* (2008) prepared the MCM-48 zeolite membrane on the pre-treated  $\alpha$ -Al<sub>2</sub>O<sub>3</sub> tubular support by hydrothermal treatment technique and applied for gas permeations. Liu *et al.* (2007) reported the preparation MCM-48 on  $\alpha$ -Al<sub>2</sub>O<sub>3</sub> ceramic tube and performed the single gas permeation tests. Guillou *et al.* (2009) developed the FAU-type zeolite membrane by in situ seeding on a multi-layer  $\alpha$ -Al<sub>2</sub>O<sub>3</sub> support and utilized for the separation of CO<sub>2</sub>/N<sub>2</sub>.

It is noteworthy to point out that the most of the prepared zeolite membranes were fabricated on  $\alpha$ -alumina support, which is restricted in industrial applications due to its higher cost. Zeolite membranes were predominantly utilized for gas phase separation applications and very limited works reported in the literature on liquid phase separation using zeolite membranes. In comparison to other zeolites such as analcime-C, silicate-1, MFI and ZSM-5, the synthesis temperature for MCM-41 is relatively lower (110°C) (Jia *et al.* 1994). Also, MCM-41 possesses a good charge density and high degree of pore symmetry, due to which it is expected to act as an ideal candidate for Fe<sup>3+</sup> separation. Therefore, this work attempts to prepare MCM-41 membrane on low cost porous ceramic support by hydrothermal treatment and investigate its performance in separation of FeCl<sub>3</sub> from aqueous solution.

## 2. Materials and methods

### 2.1 Materials

The starting materials utilized for the fabrication of the membrane support (kaolin, quartz, ball clay, pyrophyllite, and feldspar) was of mineral grade and obtained in the vicinity (Kanpur, India). Calcium carbonate, tetraethyl orthosilicate (TEOS), polyvinyl alcohol (PVA), sodium hydroxide and Iron(III) chloride (FeCl<sub>3</sub>) were procured from Merck (I), Mumbai. Cetyltrimethyl ammonium bromide (CTAB) was acquired from Central Drug House (P) Ltd., Mumbai. Cetyltrimethyl ammonium bromide (CTAB) was purchased from Sisco Research Laboratories Pvt. Ltd., Mumbai.

### 2.2 Hydrothermal synthesis of MCM-41-ceramic composite membrane

The protocol adopted to fabricate the low cost porous disk shaped ceramic supports was

reported in our earlier publication (Monash and Pugazhenthil 2011). The requisite amount of precursors (kaolin, ball clay, feldspar, quartz, calcium carbonate and pyrophyllite) was mixed together with 4 ml of PVA solution (2 wt.%) in a ball mill. Then the appropriate amount of well mixed raw materials was subjected to uni-axial pressing at 50 MPa to obtain a disk shaped supports. Subsequently, the obtained supports were subjected to the sintering process at a heating rate of 2°C/min and sintered at 950°C for 6 h in a muffle furnace after proper drying. Finally, the fabricated supports were shaped using abrasive paper and rinsed with water in sonicator followed by drying at 100°C.

MCM-41 was used as a coating material for the membrane layer. It was prepared by the hydrothermal technique reported elsewhere (Basumatary *et al.* 2015a). The gel mixture with molar composition of 1TEOS:0.1CTAB:0.3NaOH:60H<sub>2</sub>O was synthesised and transferred to Teflon lined stainless steel autoclave reactor, which contained porous ceramic disk at the bottom. After that, the tightly closed autoclave reactor was subjected to hydrothermal treatment under the static condition at 110°C for 96 h. After treatment, the membrane and MCM-41 powder were taken out from the autoclave reactor and extensively washed using Millipore water (Millipore water system ELIX-3) followed by drying at 100°C for 24 h. To eliminate the organic template from the zeolite channels, the membrane was calcined at 550°C for 5 h in an air atmosphere at a heating rate of 0.5°C/min. The stated procedure repeated for three times to deposit more quantity of MCM-41 on the support disk. After three cycle of coating, no significant weight increment was noticed and hence, the coating stopped after third coating.

### 2.3 Characterization

Different techniques were used to investigate the properties of MCM-41 zeolite membrane as well as MCM-41 powder. The structure of MCM-41 was determined by X-ray diffraction (XRD) using a Bruker A8 advance instrument working with Cu K $\alpha$  radiation sources ( $\lambda = 1.54056 \text{ \AA}$ ). The profiles were recorded in the  $2\theta$  ranges of 1 to 10° with a scan rate of 0.01°/s. The thermal behavior of MCM-41 powder was studied by thermogravimetric analysis (TGA) using Netzsch TG 209F1 Libra instrument in an air atmosphere from 30 to 950°C in 150  $\mu$ L platinum crucibles with a heating rate of 10°C/min. The morphological investigations were carried out with a field emission scanning electron microscope (FESEM, Zeiss Sigma instrument). A small size of the membrane sample was fixed on top of the stub and layered with gold using an auto fine coating instrument (JEOL JFC-1300) preceding to morphology assessment.

The porosity of the membrane was measured by utilizing water as a soaking agent (Basumatary *et al.* 2015a, b). Firstly, the dry mass ( $M_D$ ) of the membrane was determined after drying the membrane in a hot air oven at 110°C for 6 h. Then, the mass of the wet membrane ( $M_W$ ) was measured when all pores are filled with water under vacuum. After that, the mass of water saturated membrane ( $M_A$ ) was measured when the membrane was immersed in water (A refers to Archimedes). The porosity ( $\epsilon$ ) of the membrane was computed using the following relation.

$$\epsilon = \frac{M_W - M_D}{M_W - M_A} \quad (1)$$

In order to determine the pore size and permeability, the water permeation test was carried out at various applied pressures 69-483 kPa (5-32 psi) using in-house made setup as shown in Fig. 1.

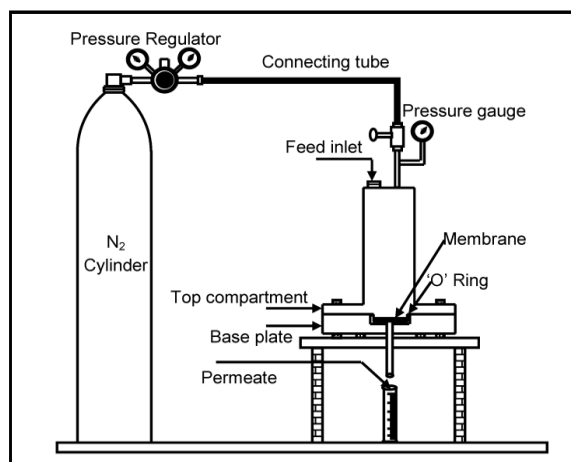


Fig. 1 Schematic representation of batch filtration setup

During each run of the experiment at different applied pressure, the permeation chamber was poured with 150 ml of Millipore water. The initial 50 ml of water passed through the membrane was thrown away and the time required for the next 50 ml of water across the membrane was considered for calculation of water flux and permeability. The pure water flux ( $J_w$ ) at a certain operating pressure can be determined from the following relation (Kumar *et al.* 2015b)

$$J_w [\text{flux}] = \frac{Q [\text{volume of water permeated, m}^3]}{A [\text{area, m}^2] \times t [\text{time, s}]} \quad (2)$$

The water permeability ( $L_h$ ) is determined from the slope of the pure water flux ( $J_w$ ) versus applied pressure across the membrane ( $\Delta P$ ). The average pore size is determined using Hagen Poiseuille expression by assuming pores are cylindrical in shape (Kumar *et al.* 2015c)

$$J_w = \frac{\epsilon r^2 \Delta P}{8 \mu \tau l} = L_h \Delta P \quad (3)$$

where,  $\epsilon$  is the porosity of the membrane,  $r$  is the pore radius of the membrane,  $l$  is assumed to be thickness of the membrane,  $\tau$  is the tortuosity factor ( $\tau = 1$ ),  $\mu$  is the viscosity of water,  $L_h$  is water permeability and  $\Delta P$  is the applied pressure.

#### 2.4 Separation experiments

The performance evaluation of the fabricated composite membrane was carried out by filtration of  $\text{Fe}^{3+}$  solution at room temperature ( $25^\circ\text{C}$ ) using dead-end filtration setup (see Fig. 1). The various concentration of  $\text{Fe}^{3+}$  solution was prepared using Millipore water and 100 mL of solution was poured into the permeation cell for each experimental run. The initial 10 ml of permeate passed through the membrane was thrown away and the time required for the next 10 ml of permeate across the membrane was collected and considered for measurement of permeate flux and concentration. Conductivity measurement (Eutech Instruments, Model: CON 2700) was used

for the determination of  $\text{Fe}^{3+}$  concentration in permeate and feed. The ultrafiltration of  $\text{Fe}^{3+}$  salt was performed at various operating conditions, such as applied pressures of 207 - 483 kPa, initial feed concentrations of 250 - 3000 ppm and pH of 2 - 5. Dilute NaOH and HCl solutions were used to adjust the pH of the salt solution.

The membrane was thoroughly rinsed by passing Millipore water at higher pressure after each experimental run. After cleaning, the water flux of the membrane was evaluated to assure about negligible flux decrement owing to the partial plugging of membrane pores. The full recuperation of the membrane was inspected by calculating the membrane hydraulic permeability equal to the actual hydraulic permeability or within the limits of  $\pm 2\%$  of actual permeability.

The observed rejection was determined by the following expression (Basumatary *et al.* 2015b)

$$R [\text{rejection, (\%)}] = 1 - \frac{C_p [\text{concentration in permeate}]}{C_f [\text{concentration in feed}]} \times 100 \quad (4)$$

### 3. Results and discussion

#### 3.1 Characterization of MCM-41 powder

Fig. 2 illustrates the powder XRD pattern of MCM-41 zeolite with high crystallinity and the obtained profile is in good agreement with patterns of MCM-41 zeolites by existence of (1 0 0), (1 1 0) and (2 0 0) diffraction peaks (Liou 2011, Udayakumar *et al.* 2005). The XRD patterns show an intense diffraction (1 0 0) peak and three higher order peaks, (1 1 0), (2 0 0), (2 1 0) at  $2\theta$  values below  $10^\circ$ , demonstrating the characteristics of MCM-41 materials (Liou 2011, Udayakumar *et al.* 2005).

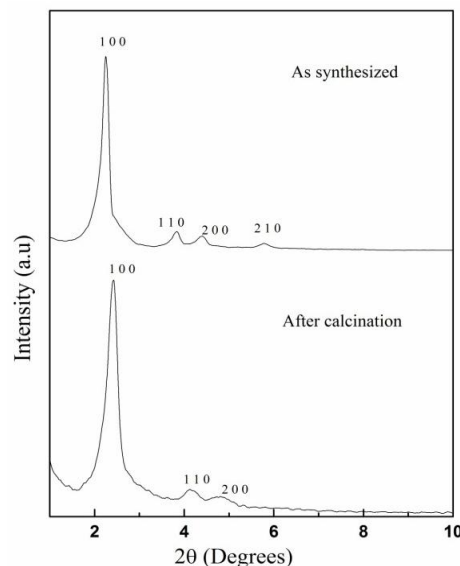


Fig. 2 XRD profile of MCM-41 powder

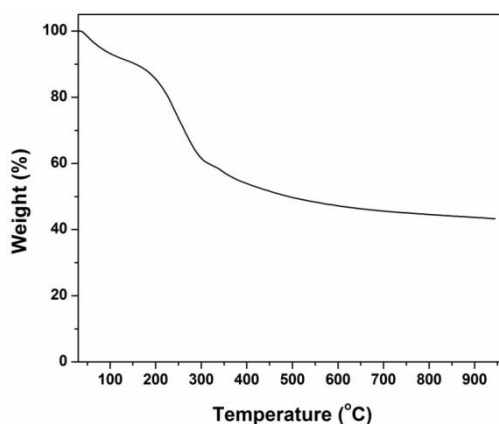


Fig. 3 TGA curve of as-synthesized MCM-41 powder

The thermogravimetric (TGA) analysis curve of the MCM-41 zeolite is displayed in Fig. 3. The sample depicts the mass decrement in three different stages. The weight loss (4-5%) below 150°C is attributed to the loss of water molecules present in the framework of the zeolite. The second stage of weight loss (36%) occurred between 150 to 320°C is most likely due to decomposition of the surfactant and intrazeolite water desorption. The third stage of weight loss (2%) at above 550°C is due to the liberation of vicinal silanol and germinal groups from the sample and no further significant weight loss is noticed.

FESEM was used to analyze surface morphology of both ceramic support and MCM-41 membrane and the obtained FESEM images are depicted in Figs. 4(a) and (b). Fig. 4(a) displays the uniform surface of the support with no cracks Fig. 4(b) shows that the synthesized MCM-41 particles are homogeneously deposited on the surface of the support. In the zeolite deposition process, the layer of MCM-41 zeolite particles completely covers the ceramic support. The overall surface morphological analysis resembles that there is no crack on the surface of the membrane. The MCM-41 zeolite material is distinctly visible in the FESEM image.

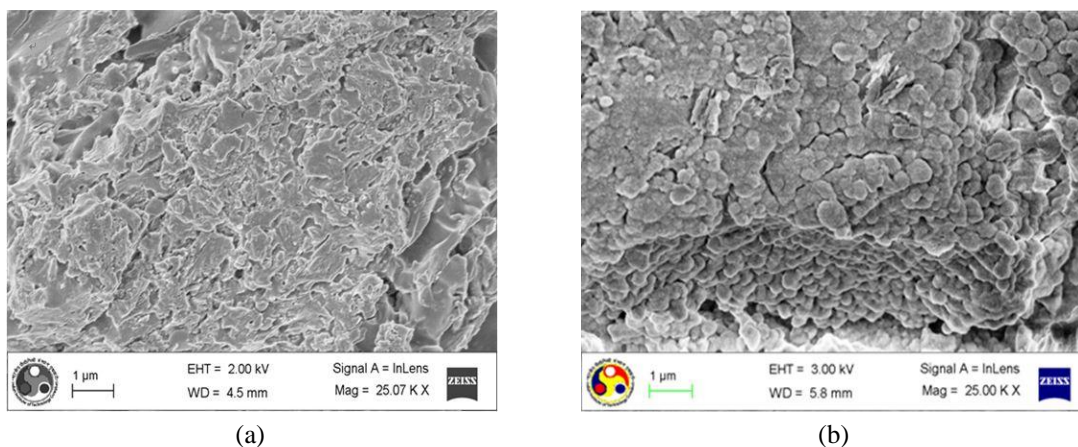


Fig. 4 FESEM images (a) support; and (b) MCM-41 composite membrane

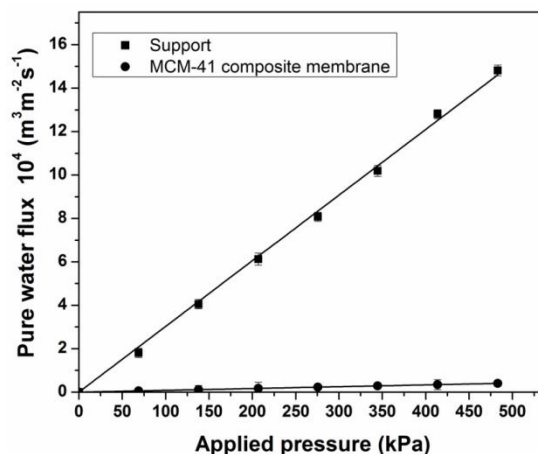


Fig. 5 Pure water flux of support and MCM-41 composite membrane

Fig. 5 illustrates the water flux of the ceramic support and zeolite membrane as a function of applied pressure. It can be noticed that the water flux increases linearly with an increase in applied pressures (69-483 kPa). This stipulates that the variation in pressure is the barely driving force for permeation. For transportation operation exclusively by convection, the flow rate is proportionate to the pressure, and is in accordance with Darcy's law.

The porosity of ceramic support and MCM-41 membrane is found to be 47% and 23%, respectively (Basumatary *et al.* 2015a). The hydraulic permeability ( $L_h$ ) of the ceramic support and zeolite membrane is calculated as  $3.63 \times 10^{-6} \text{ m}^3/\text{m}^2\text{s kPa}$  and  $6.05 \times 10^{-8} \text{ m}^3/\text{m}^2\text{s kPa}$ , respectively. Workneh and Shukla (2008) reported hydraulic permeability value for sodalite octahydrate zeolite-clay composite membrane as  $7.50 \times 10^{-8} \text{ m}^3/\text{m}^2\text{s kPa}$ . In another study, the values of hydraulic permeability determined were  $7.94 \times 10^{-8}$ ,  $5.54 \times 10^{-8}$  and  $3.89 \times 10^{-8} \text{ m}^3/\text{m}^2\text{s kPa}$  for unmodified, nitrated and aminated zeolite composite membranes, respectively by Shukla and Kumar (2007). It is apparent that the water permeability of the prepared MCM-41 zeolite membrane is higher than that of others membranes reported in the literature (Workneh and Shukla 2008, Shukla and Kumar 2007). The average pore size of the ceramic support and zeolite membrane is calculated to be  $1.0 \mu\text{m}$  and  $0.173 \mu\text{m}$ , respectively. As stated above, the porosity, water permeability and mean pore size of zeolite membrane are decreased, which is obviously due to the incorporation of the zeolite layer on the ceramic substrate by hydrothermal treatment.

### 3.2 Ultrafiltration of $\text{Fe}^{3+}$ salt solution

The fabricated MCM-41 ceramic composite membrane was applied for the separation of  $\text{Fe}^{3+}$  present in aqueous medium. Applied pressure, initial feed concentration and pH of solution are the important variables that influence the filtration process in terms of permeate flux and rejection. Hence, the effect of these parameters was investigated in ultrafiltration of  $\text{Fe}^{3+}$  salt solution.

#### 3.2.1 Influence of applied pressure

Fig. 6 illustrates the permeate flux and rejection profiles for various applied pressure (207-483 kPa) for a fixed  $\text{Fe}^{3+}$  salt concentration of 3000 ppm and natural pH of solution (2.45). It can be

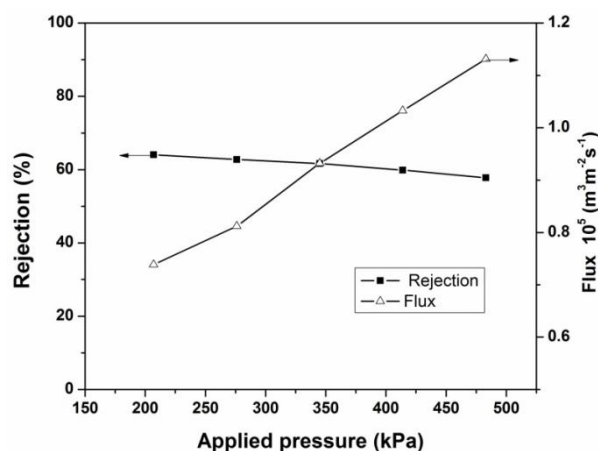


Fig. 6 Influence of applied pressure on permeate flux and rejection

inferred from Fig. 6 that the presence of  $Fe^{3+}$  ions offers an extra resistance to the flow due to which the permeate flux is lower than that of water flux. The permeate flux of the salt solution also depends upon the electrostatic interaction between the membrane surface and an electrolyte, thereby providing an additional resistance to the flow through the membrane. It is noticed from Fig. 6 that the rejection exhibits a decreasing trend with an increment of pressure because of severe concentration polarization caused by the enhanced accumulation of  $Fe^{3+}$  ions on the surface of the membrane at elevated pressure (Shukla and Kumar 2005). As a result, the permeate concentration increases owing to increase in the convective flux. Besides, the additional factors such as membrane charge density and interaction between ionic solute and charge of the membrane are influencing too in rejection. In this parameter study, the maximum rejection of  $Fe^{3+}$  is observed to be 64% for the MCM-41 composite membrane at applied pressure of 207 kPa.

### 3.2.2 Influence of initial feed concentration

Fig. 7 demonstrates the variation of permeate flux and rejection profiles for various feed concentrations (250-3000 ppm) at applied pressure of 276 kPa and natural pH of the solution (2.45). It is evident from this figure that there is a decline in the flux when the salt concentration gradually increases. This is probably due to enhancement of concentration polarization and occurrence of incomplete plugging of membrane pores. The observed rejection displays a decreasing trend with increasing salt concentration, as illustrated in Fig. 7. This is regular trend especially for membrane holds charge and it is observed due to lowering of effective charge at higher feed concentration (Shukla and Kumar 2005). Besides, Donnan exclusion also acts considerable part for decrement in rejection with increasing concentration of the salt (Chung *et al.* 2005). The concentration at the surface of the membrane increases with increasing salt concentration, causing severe concentration polarization. In the studied concentration ranges, the highest percentage of rejection 71% is obtained for the feed concentration of 250 ppm at applied pressure of 276 kPa.

### 3.2.3 Influence of pH

Fig. 8 shows the variation of permeate flux and rejection profile with pH of the solution. It can be observed that the flux tends to increase as pH of the solution augments from 2 to 4.0, due to



decreased electro-viscous effect. The magnitude of the surface potential of the composite membrane reduces at higher pH values, closer to its iso-electric point (IEP) (pH: 3.9) (Basumatary *et al.* 2015a). The permeate flux seems to decrease with an increase in the pH from 4 to 5.0 (beyond to IEP). Considering electro-viscous effect, the permeate flux is expected to attain its maximum value at the IEP of the membrane.

The observed rejection of  $\text{Fe}^{3+}$  decreases with raising the pH from 2.0 to 4.0 because the membrane surface interaction with  $\text{Fe}^{3+}$  ions varies at different pH values. When an electrolyte solution is in contact with a charged membrane, there is a generation of potential difference, termed as Donnan potential, due to the difference in ionic concentration in membrane surface and solution. The co-ions, with similar charge as that of the membrane, will be higher in concentration in the solution than that near the membrane surface, whereas the concentration of the counter-ions (ions with the opposite charge) will be higher near the membrane surface than in the solution. The Donnan potential generated at the membrane - solution interface maintains an electrochemical equilibrium, facilitating the repulsion of co-ions by the membrane (Chung *et al.* 2005). The

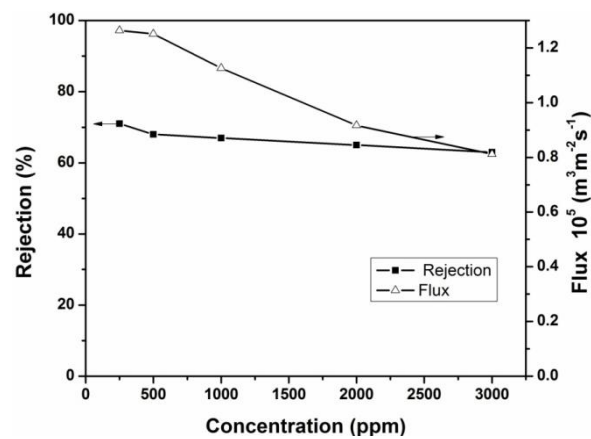


Fig. 7 Influence of concentration on permeate flux and rejection

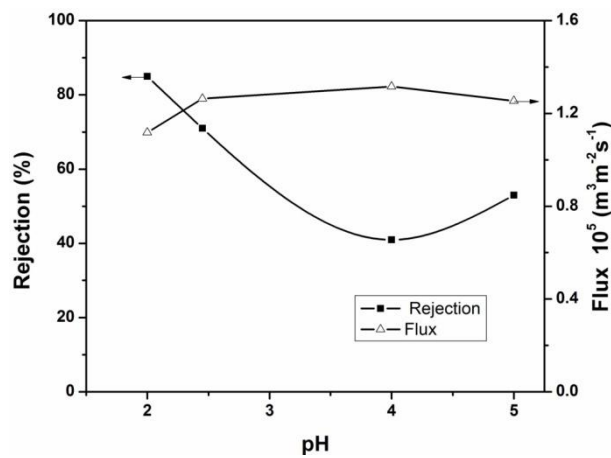


Fig. 8 Influence of pH on permeate flux and rejection

membrane surface potential decreases when pH of the solution approaches IEP of the membrane, while increasing from 2 to 4 (Nazzal and Wiesner 1994). Thus the repulsion between the positively charged membrane and  $\text{Fe}^{3+}$  ions decreases, thereby reducing the rejection of  $\text{Fe}^{3+}$  ions. Subsequently,  $\text{Cl}^-$  ions are also rejected in order to maintain electroneutrality, since the cation and the anion are unable to act independently (Majhi *et al.* 2009). Furthermore, it is observed that the rejection increases slightly with enhancing pH beyond IEP of the membrane. This is due to the fact, that the membrane is negatively charged at pH higher than the IEP and the surface charge (negative) of the membrane at pH 5.0 will be higher than that at pH 4.0. As a result of higher surface charge, the electrostatic repulsive intensity between the  $\text{Cl}^-$  ions and the membrane surface increases, thereby resulting in increased rejection with increasing the pH value from 4 to 5.0.

#### 4. Conclusions

MCM-41-ceramic composite membrane was effectively fabricated on an inexpensive porous disk shaped ceramic support by hydrothermal synthesis technique.

- The pore size of ceramic disk was reduced from 1.0 to 0.173  $\mu\text{m}$  with the repeated deposition of MCM-41 as the selective layer on ceramic support.
- The potential of the membrane was investigated by the ultrafiltration of  $\text{Fe}^{3+}$  from aqueous solution.
- Highest rejection of 85% is attained with the feed concentration of 250 ppm at applied pressure of 276 kPa and pH of 2.

It can be concluded that the prepared MCM-41 composite membrane has better potential for the removal of metals from aqueous solution.

#### References

- Basumatary, A.K., Kumar, R.V., Ghoshal, A.K. and Pugazhenthii, G. (2015a), "Synthesis and characterization of MCM-41-ceramic composite membrane for the separation of chromic acid from aqueous solution", *J. Membr. Sci.*, **475**, 521-532.
- Basumatary, A.K., Singh, P.V., Kumar, R.V., Ghoshal, A.K. and Pugazhenthii, G. (2015b), "Development and characterization of a MCM-48 ceramic composite membrane for the removal of Cr(VI) from an aqueous solution", *J. Environ. Eng-ASCE*, **142**(9), C4015013-11.
- Chougui, A., Zaiter, K., Belouatek, A. and Asli, B. (2014), "Heavy metals and color retention by a synthesized inorganic membrane", *Arabian J. Chem.*, **7**(5), 817-822.
- Chung, C.V., Buu, N.Q. and Chau, N.H. (2005), "Influence of surface charge and solution pH on the performance characteristics of a nanofiltration membrane", *Sci. Technol. Adv. Mater.*, **6**(3-4), 246-250.
- Guillou, F., Rouleau, L., Pirngruber, G. and Valtchev, V. (2009), "Synthesis of FAU-type zeolite membrane: An original in situ process focusing on the rheological control of gel-like precursor species", *Micropor. Mesopor. Mater.*, **119**(1-3), 1-8.
- Gzara, L. (2001), "Removal of chromate anions by micellar-enhanced ultrafiltration using cationic surfactants", *Desalination*, **137**(1-3), 241-250.
- Jia, M.D., Chen, B., Noble, R.D. and Falconer, J.L. (1994), "Ceramic-zeolite composite membranes and their application for separation of vapor/gas mixtures", *J. Membr. Sci.*, **90**(1-2), 1-10.
- Kasim, N., Mohammad, A.W. and Abdullah, S.R.S. (2016), "Performance of membrane filtration in the removal of iron and manganese from Malaysia's groundwater", *Membr. Water Treat., Int. J.*, **7**(4), 277-

- 296.
- Kumar, R.V., Moorthy, I.G. and Pugazhenth, G. (2015a), "Modelling and optimization of critical parameters by hybrid RSM-GA for the separation of BSA using tubular configured MFI-type zeolite microfiltration membrane", *RSC Adv.*, **5**(106), 87645-87659.
- Kumar, R.V., Basumatary, A.K., Ghoshal, A.K. and Pugazhenth, G. (2015b), "Performance assessment of an analcime-C zeolite-ceramic composite membrane by removal of Cr (VI) from aqueous solution", *RSC Adv.*, **5**, 6246-6254.
- Kumar, R.V., Ghoshal, A.K. and Pugazhenth, G. (2015c), "Elaboration of novel tubular ceramic membrane from inexpensive raw materials by extrusion method and its performance in microfiltration of synthetic oily wastewater treatment", *J. Membr. Sci.*, **490**, 92-102.
- Liou, T.H. (2011), "A green route to preparation of MCM-41 silicas with well-ordered mesostructure controlled in acidic and alkaline environments", *Chem. Eng. J.*, **171**(3), 1458-1468.
- Liu, C., Wang, L., Ren, W., Rong, Z., Wang, X. and Wang, J. (2007), "Synthesis and characterization of a mesoporous silica (MCM-48) membrane on a large-pore  $\alpha$ -Al<sub>2</sub>O<sub>3</sub> ceramic tube", *Micropor. Mesopor. Mater.*, **106**(1-3), 35-39.
- Majhi, A., Monash, P. and Pugazhenth, G. (2009), "Fabrication and characterization of  $\gamma$ -Al<sub>2</sub>O<sub>3</sub>-clay composite ultrafiltration membrane for the separation of electrolyte from its aqueous solution", *J. Membr. Sci.*, **340**(1-2), 181-191.
- Monash, P. and Pugazhenth, G. (2011), "Development of ceramic supports derived from low-cost raw materials for membrane applications and its optimization based on sintering temperature", *Int. J. Appl. Ceram. Technol.*, **8**(1), 227-238.
- Nandi, B.K., Uppaluri, R. and Purkait, M.K. (2008), "Preparation and characterization of low cost ceramic membranes for micro-filtration applications", *Appl. Clay Sci.*, **42**(1-2), 102-110.
- Nazzal, F.F. and Wiesner, M.R. (1994), "pH and ionic strength effects on the performance of ceramic membranes in water filtration", *J. Membr. Sci.*, **93**(1), 91-103.
- Shukla, A. and Kumar, A. (2005), "Characterization of chemically modified zeolite-clay composite membranes using separation of trivalent cations", *Sep. Purif. Technol.*, **41**(1), 83-89.
- Shukla, A. and Kumar, A. (2007), "Separation of Cr(VI) by zeolite-clay composite membranes modified by reaction with NO<sub>x</sub>", *Sep. Purif. Technol.*, **52**(3), 423-429.
- Udayakumar, S., Pandurangan, A. and Sinha, P.K. (2005), "Mesoporous material as catalyst for the production of fine chemical: Synthesis of dimethyl phthalate assisted by hydrophobic nature MCM-41", *J. Mol. Catal. A: Chem.*, **240**(1-2), 139-154.
- Urbanowska, A. and Kabsch-Korbutowicz, M. (2016), "Cleaning agents efficiency in cleaning of polymeric and ceramic membranes fouled by natural organic matter", *Membr. Water Treat., Int. J.*, **7**(1), 1-10.
- Wang, Z., Kumakiri, I., Tanaka, K., Chen, X. and Kita, H. (2013), "NaY zeolite membranes with high performance prepared by a variable-temperature synthesis", *Micropor. Mesopor. Mater.*, **182**, 250-258.
- Workneh, S. and Shukla, A. (2008), "Synthesis of sodalite octahydrate zeolite-clay composite membrane and its use in separation of SDS", *J. Membr. Sci.*, **309**(1-2), 189-195.
- Wu, S., Yang, J., Lu, J., Zhou, Z., Kong, C. and Wang, J. (2008), "Synthesis of thin and compact mesoporous MCM-48 membrane on vacuum-coated  $\alpha$ -Al<sub>2</sub>O<sub>3</sub> tube", *J. Membr. Sci.*, **319**(1-2), 231-237.